

## Article

# Computer-Aided Slope Stability Analysis of a Landslide—A Case Study of Jhika Gali Landslide in Pakistan

Muhammad Nasir Amin <sup>1,\*</sup>, Muhammad Umair Ashfaq <sup>2,\*</sup>, Hassan Mujtaba <sup>3</sup>, Saqib Ehsan <sup>2</sup>, Kaffayatullah Khan <sup>1</sup> and Muhammad Iftikhar Faraz <sup>4</sup>

<sup>1</sup> Department of Civil and Environmental Engineering, College of Engineering, King Faisal University, Al-Ahsa 31982, Saudi Arabia

<sup>2</sup> Department of Civil Engineering, NFC Institute of Engineering and Fertilizer Research, Faisalabad 38090, Pakistan

<sup>3</sup> Department of Civil Engineering, University of Engineering and Technology, Lahore 54000, Pakistan

<sup>4</sup> Department of Mechanical Engineering, College of Engineering, King Faisal University, Al-Ahsa 31982, Saudi Arabia

\* Correspondence: mgadir@kfu.edu.sa (M.N.A.); umairashfaq@iefr.edu.pk (M.U.A.); Tel.: +966-13-589-5431 (M.N.A.); Fax: +966-13-581-7068 (M.N.A.)

**Abstract:** The present research study has been undertaken to carry out slope stability evaluation of the Jhika Gali landslide in Pakistan using GeoStudio. For this purpose, the site geometry of the existing slope adjacent to the slided one was measured and samples were collected from the site. The in-situ moisture content was 14% and dry unit weight was 18.63 kN/m<sup>3</sup>. Unconfined compression tests and unconsolidated-undrained (UU) triaxial tests were performed on samples reconstituted at in-situ dry unit weight, standard Proctor and modified Proctor maximum dry unit weights. The test results show that the shear strength and deformation parameters, i.e., undrained shear strength, angle of internal friction and deformation modulus decreased from 200 kPa to 90 kPa, 23° to 12° and 51 MPa to 32 MPa, respectively, with an increase in the percentage of saturation from 35% to 95% at a specific dry unit weight. The slope was also modeled in GeoStudio for limit equilibrium analysis, and slope stability analysis was performed using the values of undrained shear strength and the angle of internal friction as determined in the laboratory at varying degrees of saturation. The limit equilibrium analysis showed that the factor of safety reduces from 1.854 to 0.866 as the saturation of material increases from 35% to 95%. The results also suggest that, as the percentage of saturation increases above 85%, the soil loses its shear strength significantly and gains in bulk unit weight, so at this stage the material starts sliding. Additionally, slope stability analysis was carried out by changing the slope geometry in three different ways, i.e., by reducing the height of the slope, adding a counterweight at the toe of the slope and by making benches on the slope. The results of GeoStudio analysis showed that the slope will be stable even above 85% degree of saturation.

**Keywords:** landslide; degree of saturation; GeoStudio; undrained shear strength ( $c_u$ ); limit equilibrium analysis; angle of internal friction ( $\phi$ )



**Citation:** Amin, M.N.; Umair Ashfaq, M.; Mujtaba, H.; Ehsan, S.; Khan, K.; Faraz, M.I. Computer-Aided Slope Stability Analysis of a Landslide—A Case Study of Jhika Gali Landslide in Pakistan. *Sustainability* **2022**, *14*, 12954. <https://doi.org/10.3390/su142012954>

Academic Editors: Danqing Song, Zhuo Chen, Mengxin Liu and Yutian Ke

Received: 31 August 2022

Accepted: 30 September 2022

Published: 11 October 2022

**Publisher's Note:** MDPI stays neutral with regard to jurisdictional claims in published maps and institutional affiliations.



**Copyright:** © 2022 by the authors. Licensee MDPI, Basel, Switzerland. This article is an open access article distributed under the terms and conditions of the Creative Commons Attribution (CC BY) license (<https://creativecommons.org/licenses/by/4.0/>).

## 1. Introduction

Landslides are a part of the natural evolution of landscapes that happen all over the world on a regular basis [1]. Landslides are usually triggered on natural slopes, but they may also occur on man-made slope. Landslides cause several hazards, including damage to roads, utilities, and natural river courses, as well as the loss of human life. Prior information of the causative factors is important for risk identification and mitigation. In Pakistan's northern regions, landsliding is a major concern. Natural slopes present at various locations in northern areas are prone to landslides which occur frequently during rainy seasons (rainfall infiltration being the most significant during the monsoon period) every year [2]. Many other factors also contribute to these events including fragile geology, high seismicity,

and active faulting. These calamities have caused casualties and considerable financial loss to public and personal properties each year. A similar event occurred during the excavations for the parking plaza at Jhika Gali, where the landslide resulted in damage to the road structure and personal property. A consequential and practically sound attitude is required to minimize and mitigate the disastrous effects of landsliding in these areas. The shear strength of the landslide matrix material is important for slope stability [3]. The soil-like materials draw their shear strength from the resistance due to the interlocking of the individual grains, sliding resistance among the soil particles and adhesion among the particles [4]. Various researchers including Santoso et al. (2011), Kawamura et al. (2013), Khattab et al. (2018), Tsai et al. (2010) in the past have studied the relationship between the shear strength and the degree/percentage of saturation for different soils [5–8].

Waseem et al. (2021) studied the slope failure at Qalandar Abad, Khyber Pakhtunkhwa, Pakistan. The determination of the factor of safety (FOS) for slope stability was carried out with the Limit Equilibrium Method (LEM) on GeoStudio Software. The Bishop, Morgenstern-Price, Janbu, and ordinary slice methods were assumed to analyze dry and fully saturated field drainage conditions in the SLOPE/W program of the software. For the Gravity Loading condition, the FOS ranged from 0.344 to 0.383. In the seismic loading condition, the FOS ranged from 0.287 to 0.332. The values of FOS indicated that the slopes are unstable, which is the primary cause of slope failure incidents in Qalandar Abad. For stability purposes, a retaining wall was provided to strengthen the slope. After strengthening the slope, the FOS increased from 1.531 to 1.690 for gravity loading, whereas the FOS for seismic loading increased from 1.293 to 1.482. Moreover, it was concluded that with the increase in friction angle and soil cohesiveness, the FOS increases. In contrast, the FOS decreases when there is an increase in overburden pressure and the unit weight of soil [9].

Pasierb et al. (2019) investigated the current landslide conditions in Brzozówka, Poland, and focused on how different soil saturations affect landslide stability. Information on the geological structure and geotechnical parameters of the landslide as provided by a combination of geophysical and geotechnical testing were used in landslide stability computational simulations in which a two-phase model (soil and water) was assumed to include the effective parameters of soil strength and transient flow conditions as well as a partial saturation region. The method of electric resistivity tomography (ERT) revealed that the sliding surface obtained from numerical modelling was nearly smooth. When the upper part of the slope was saturated to more than 80%, the landslide occurred, according to the evidence [10].

Yanrong (2018) investigated the shear strength of Malan Loess in China and found that at 7% moisture content the shear strength parameters, i.e., ( $c$  and  $\phi$ ) are at their peak; the values of these parameters reduce to 20% moisture content and after this cohesion reduces drastically and material starts to slide [11].

Xu et al. (2018) studied the saturation effect on the shear strength of Loess with respect to the structure of the soil. Triaxial and oedometer tests were conducted on in-situ and remolded samples of soil in a saturated condition. The behavior of soil particles is strongly affected by its structure. However, with the increase in degree of saturation both soils show drastic change in shear strength and the shear strength of these soils reduces quickly as the water content increases. This loss in shear strength may cause the initiation of relative movement of soil particles and cause landslides [12].

Zhang et al. (2016) determined the mechanism of failure of red mudstone landslides by performing a direct shear test. They concluded that due to rainwater infiltration in mudstone the shear strength reduces. The test results indicated that with the increase in degree of saturation from 48% to 100% the value of cohesion of mudstone decreased by 26% and the angle of internal friction of mudstone decreased by 52%. In addition, immersion of samples in water for 16 days at the same degree of saturation reduced the angle of internal friction and cohesion by 69% and 77%, respectively [13].

Ali et al. (2016) studied the Murree Kohala Road landslides in Pakistan and investigated the impact of saturation and bulk density on the failure surfaces. According to

the results of compression tests, the unconfined compression strength of soil decreases as the percentage of saturation rises and increases as the density increases. Similarly, UU triaxial test results showed that as the percentage of saturation increases values of cohesion and the angle of internal friction of soil decreases; the two are indirectly related. The analysis revealed that the shear strength of the soil matrix decreased with an increment in the percentage of saturation and the slope became critical around 65% to 70% degrees of saturation [14].

Ahmad et al. (2016) studied the failure analysis of the Havelian landslide in Pakistan which was triggered by rainfall. A number of direct shear tests were carried out on reconstituted samples at in-situ landslide matrix material density with different degrees of saturation to determine the effect on the mobilized shear strength. Finally, using shear strength parameters, i.e., ( $c$  and  $\phi$ ) at different degrees of saturation, the FOS along the likely surface failure was calculated using the Slope/W software. The study found that as the soil matrix degree of saturation increased, the shear strength decreased, and the slope became critical at about 50% saturation [15].

Ali et al. (2014) studied the landslides and noted that failures occur along an impenetrable boundary which is present at a specific depth. But in reality, failure can occur along any depth. By performing different stability and seepage analyses, they observed the effect of boundary conditions on landslides. In these analyses, they varied the rainfall intensities and studied the time of failure, mechanism of failure, and depth of failure. They observed that the conditions mentioned above are important factors for the initiation of landslides [16].

Li et al. (2013) studied the combined effect of precipitation and permeability characteristics on the failure mechanism of slopes of homogenous soil. They concluded that precipitation and permeability impact the steadiness of slopes heavily because of an increase in the degree of saturation. They also showed that as the slope angle ( $\alpha$ ) increases from the angle of internal friction ( $\phi$ ) of the soil, failure plane propagation starts in the wetting front of the slope [17].

A landslide was triggered along Jhika Gali road which caused disruption to the road network. The current research is focused on investigating the slope failure along the Jhika Gali road to estimate the shear strength of the soil along with deformation characteristics under different degrees of saturation. In addition, slope stability analysis was carried out by changing the slope geometry and the results revealed that flattening reduces the risk of a landslide even at 85% degree of saturation. The findings will be beneficial to predict slope stability based on shear strength parameters at different degrees of saturation.

## 2. Materials and Methods

### 2.1. Soil Sample Collection

The Jhika Gali site (33°54'54.72" N, 73°25'8.76" E) was visited during April 2019 and sample collection, including measurement of the approximate geometry of the existing slope by using a total station, was noted. The investigated slope had a height of about 65 m and width of almost 95m from the toe and is shown in Figure 1. It was also observed that the slopes of the failure surface ranged between 30 and 45 degrees. Slided material present at the site was reddish in color and became sticky with the addition of water indicating the presence of high clay content in the sample. It was also observed that the slided mass consisted of small particles as well as large boulder-size particles. In this regard, two different points were selected to check the homogeneity of the material and the material consisting of lumps of slided material were excavated from the surface of the landslide and brought to the laboratory for investigations. The material was dried and pulverized to get the samples ready for laboratory testing.

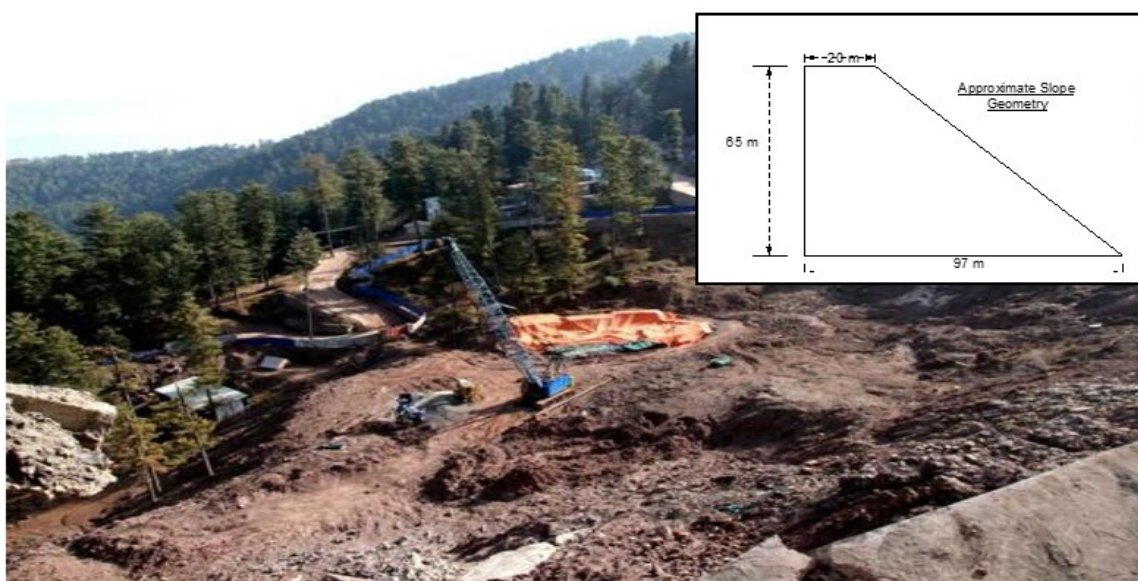


**Figure 1.** Jhika Gali landslide site.

## 2.2. Soil Sample Properties

The physical and engineering properties of the soil were evaluated using classification tests, standard Proctor and modified Proctor tests, and the findings are summarized in Table 1. The result of particle size analysis is shown in Figure 2.

**Table 1.** Summary of index properties of slid material.

Sr. No.	Description	Result
1	Gravel (%)	1
2	Sand (%)	21
3	Silt (%)	43
4	Clay (%)	35
5	Liquid Limit, LL (%)	38
6	Plastic Limit, PL (%)	23
7	Plasticity Index, PI	15
8	Specific Gravity, G <sub>s</sub>	2.72
9	USCS Classification	CL
10	AASHTO Classification	A-6(6)
11	Standard Proctor dry unit weight at OMC 10.94%	18.14 kN/m <sup>3</sup>
12	Modified Proctor dry unit weight at OMC 9.5%	20.31 kN/m <sup>3</sup>

The slid material has 1% gravel size particles (coarser than 4.75 mm), 21% sand size particles (finer than 4.75 mm and coarser than 0.075 mm) while the remaining 78% are fines (finer than 0.075 mm) out of which 35% are clay size particles (finer than 0.005 mm) and 43% are silt size particles (finer than 0.075 mm and coarser than 0.005 mm). The soil has a liquid limit (LL) of 38% and a plasticity index of 15%, according to the consistency limits measure. According to the unified soil classification system (USCS), the soil is categorized as lean clay with sand (CL), and it is classified as A-6 with group index 6 by AASHTO. The sample was subjected to standard Proctor and modified Proctor tests in accordance with ASTM D 698 and D 1557, yielding maximum dry unit weights of 18.14 kN/m<sup>3</sup> and 20.31 kN/m<sup>3</sup> for the sample, respectively. The in-situ dry unit weight of soil as measured by the block sample is 18.63 kN/m<sup>3</sup> [18,19].





Figure 3. Triaxial apparatus setup.



Figure 4. Tested samples at 95% degrees of saturation.

#### 2.4. Slope Stability Analysis

Slope stability analyses were performed by adopting the limit equilibrium approach in Slope/W software based on the determined shear strength parameters along the most likely failure planes. Slope/W allows a variety of methods to determine the safety factor, but in this research the Morgenstern–Price method was used due to the simple geometry of the Jhika Gali landslide and its popularity among different researchers [21]. In this method to find out the coefficient of reliability, the slipped mass is divided into a number of slices; then in each slice inter part forces and internal forces are obtained. The Morgenstern–Price method considers two reliability coefficients: one is based on the result of forces equilibrium in the horizontal direction and the second is based on the moment equilibrium.

The force equilibrium factor of safety is.

$$F_f = \frac{\sum(c' \beta \cos \alpha + (N - u \beta) \tan \phi' \cos \alpha)}{\sum N \sin \alpha + \sum kW - \sum D \cos \omega \pm \sum A}$$

where

$c'$  = effective cohesion

$\phi'$  = effective angle of friction

$u$  = pore-water pressure

$N$  = slice base normal force ( $W \cos \alpha$ )

$W$  = slice weight

$A$  = the resultant external water forces

$kW$  = the horizontal seismic load applied through the centroid of each slice

$D$  = external point load

$\beta, R, x, f, d$  = geometric parameters

$\omega$  = the angle of the point load from the horizontal. This angle is measured counter-clockwise from the positive x-axis

$\alpha$  = inclination of slice base

The moment equilibrium factor of safety is.

$$F_m = \frac{\sum(c' \beta R + (N - u \beta) R \tan \phi')}{\sum Wx - \sum Nf + \sum kW \pm \sum Df \pm \sum Aa}$$

In the above relations  $N$  is the normal force of the slice at the base and obtained from the following relation

$$N = \frac{W - \left[ \frac{c' \beta \sin \alpha + u \beta \sin \alpha \tan \phi'}{F_s} \right] + [D \sin \omega]}{\cos \alpha + \frac{\sin \alpha \tan \phi'}{F_s}}$$

where

$\lambda$  = percentage (in decimal form) of the function used

$X$  = interslice shear force

Interslice shear force is determined through the following empirical relation

$$X = E \lambda f(x)$$

where

$E$  = interslice normal force, and is determined through the following relationship

$$E_R = E_{L+} \left[ \frac{(c' \beta \sin \alpha - u \beta \tan \phi') \cos \alpha}{F_s} \right] + N \left[ \frac{\tan \phi' \cos \alpha}{F_s} - \sin \alpha \right] - kW + D \cos \omega$$

In GeoStudio modeling water seepage, the change in saturation was considered to be uniform, and the unit weight and shear strength parameters were changed correspondingly.

After entering the requisite parameters, the interstice forces were measured, allowing the factor of safety to be determined along the supposed slip surface.

### 3. Results

Previous researchers, have examined the relationship between degrees of saturation and shear strength in sandy soils [22–26]. These studies have concluded that water content within a ground mass tends to increase with the rainwater ingress depending on the extent of precipitation and is the most obvious reason for initiation of the landslide. On the basis of these results, the current study was conducted to investigate the effect of degree of saturation on shear strength parameters of the soil at Jhika Gali.

#### 3.1. Triaxial Compression Test

Unconsolidated undrained (UU) triaxial tests were performed to observe the rapid reaction of rainwater on undrained shear strength parameters of slided material to be used for slope stability analysis. All the laboratory tests were performed on the material passing through a sieve #4. Triaxial tests were performed on the remolded samples prepared at three different dry unit weights (18.14, 18.63 and 20.31 kN/m<sup>3</sup>) and degrees of saturation varying from 35–95%. Samples remolded at a specific dry unit weight and degree of saturation were tested at confining pressures of 50 kPa, 100 kPa and 150 kPa. Through these Triaxial tests shear strength parameters, i.e., the undrained shear strength and friction angle were calculated and used for slope stability analysis. In a series of triaxial tests performed at standard Proctor dry unit weight of 18.14 kN/m<sup>3</sup>, modified Proctor dry unit weight of 20.31 kN/m<sup>3</sup> and in-situ dry unit weight of 18.63 kN/m<sup>3</sup> the value of undrained shear strength ( $c_u$ ) decreased from 186.03 kPa to 89.57 kPa, 199.81 kPa to 96.46 kPa and 189 kPa to 91 kPa respectively, as the saturation increased from 35% to 95%. In the same way, in a series of triaxial tests at standard Proctor dry unit weight of 18.14 kN/m<sup>3</sup>, modified Proctor dry unit weight of 20.31 kN/m<sup>3</sup> and in-situ dry unit weight of 18.63 kN/m<sup>3</sup> the value of angle of internal friction ( $\phi$ ) decreased from 22.54° to 12.3°, 23.27° to 13.69° and 22.7° to 12.6° respectively, as the saturation increased from 35% to 95%.

A comparison of degree of saturation with undrained shear strength ( $c_u$ ) as shown in Figure 5 was used to investigate the decreasing trend with an increase in the degree of saturation at different dry unit weights. It was observed that the undrained shear strength decreased by about 51% as the saturation increased from 35% to 95%.

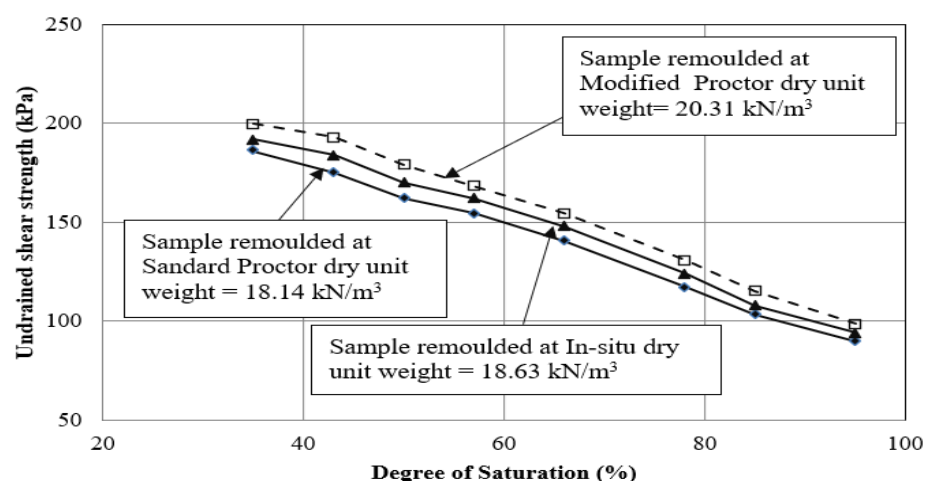
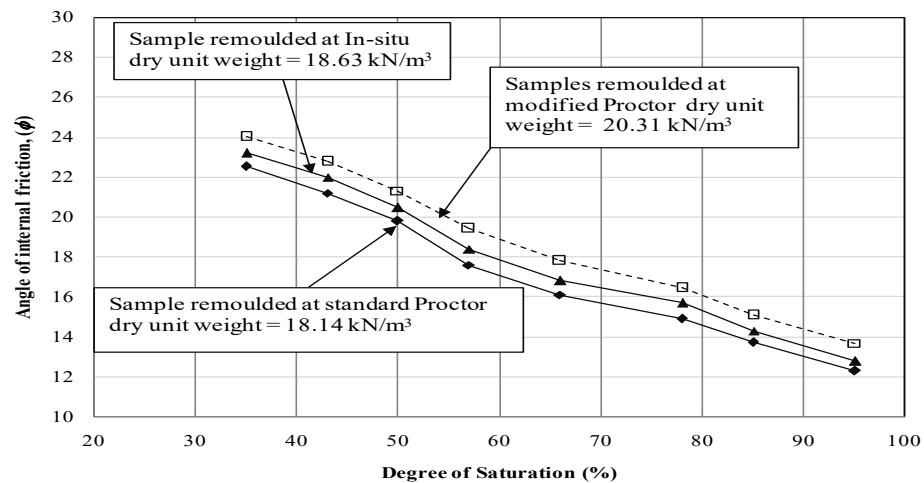


Figure 5. Degree of saturation vs. undrained shear strength of samples remolded to in-situ, standard and modified Proctor compaction energy.

Similarly, in Figure 6 the degree of saturation is compared to the angle of internal friction. It can be inferred that as the saturation rises from 35% to 95% at different dry unit weights, the friction angle of slided content decreases by about 41%.



**Figure 6.** Degree of saturation vs. friction angle of samples remoulded to in-situ, standard and modified Proctor compaction energy.

### 3.2. Unconfined Compression Test

Unconfined compression tests were carried out on remoulded samples with a diameter of 1.5 inches and a height of 3 inches in accordance with ASTM D 2166, and the deformation modulus ( $E_{50}$ ) for each sample was calculated using the axial stress versus axial strain relationship.

The relation between the axial strain and axial stress of the matrix soil remoulded at modified Proctor dry unit weight, i.e., 20.31 kN/m<sup>3</sup>, at standard Proctor dry unit weight, i.e., 18.14 kN/m<sup>3</sup> and at in-situ dry unit weight 18.63 kN/m<sup>3</sup> with the increasing degree of saturation is shown in Figure 7. In a number of unconfined compression tests carried out on samples remoulded at standard Proctor dry unit weight of 18.14 kN/m<sup>3</sup>, modified Proctor dry unit weight of 20.31 kN/m<sup>3</sup> and in-situ dry unit weight of 18.63 kN/m<sup>3</sup> the value of unconfined compression strength decreased from 707 kPa to 344 kPa, 755 kPa to 383 kPa and 718 kPa to 353 kPa, respectively, as the saturation increased from 35% to 95%. This is due to increased saturation as a result of rainfall infiltration, which leads to slope failure.

According to the test results, the material's unconfined compressive strength increases as the dry unit weight of the remoulded sample increases, but this strength reduces as the saturation increases, as shown in Figure 8. In all cases, however, loss of unconfined compression strength of about 49.3~51.3% is observed with the increasing degree of saturation.

Through this undrained shear strength, the deformation modulus of slided material as shown in the inset in Figure 7a was evaluated by using the following relation.

$$E_{50} = \frac{\sigma_{50}}{\varepsilon_{50}}$$

The summary of these results showed that  $E_{50}$  varies from 44.7 MPa to 32.2 MPa in the case of standard Proctor dry unit weight as the percentage of saturation increases from 35% to 95%. Similarly, the  $E_{50}$  value decreases from 50.8 MPa to 36.8 MPa in the case of modified Proctor dry unit weight as the percentage of saturation increases from 35% to 95%. The  $E_{50}$  value decreases from 46.1 MPa to 33.2 MPa in the case of in-situ dry unit weight as the percentage of saturation increases from 35% to 95%. Figure 9 shows the decreasing trend of deformation modulus ( $E_{50}$ ) with the increase in the saturation at in-situ dry unit weight i.e., 18.61 kN/m<sup>3</sup>, standard Proctor dry unit weight i.e., 18.14 kN/m<sup>3</sup> and modified Proctor dry unit weight 20.31 kN/m<sup>3</sup>.

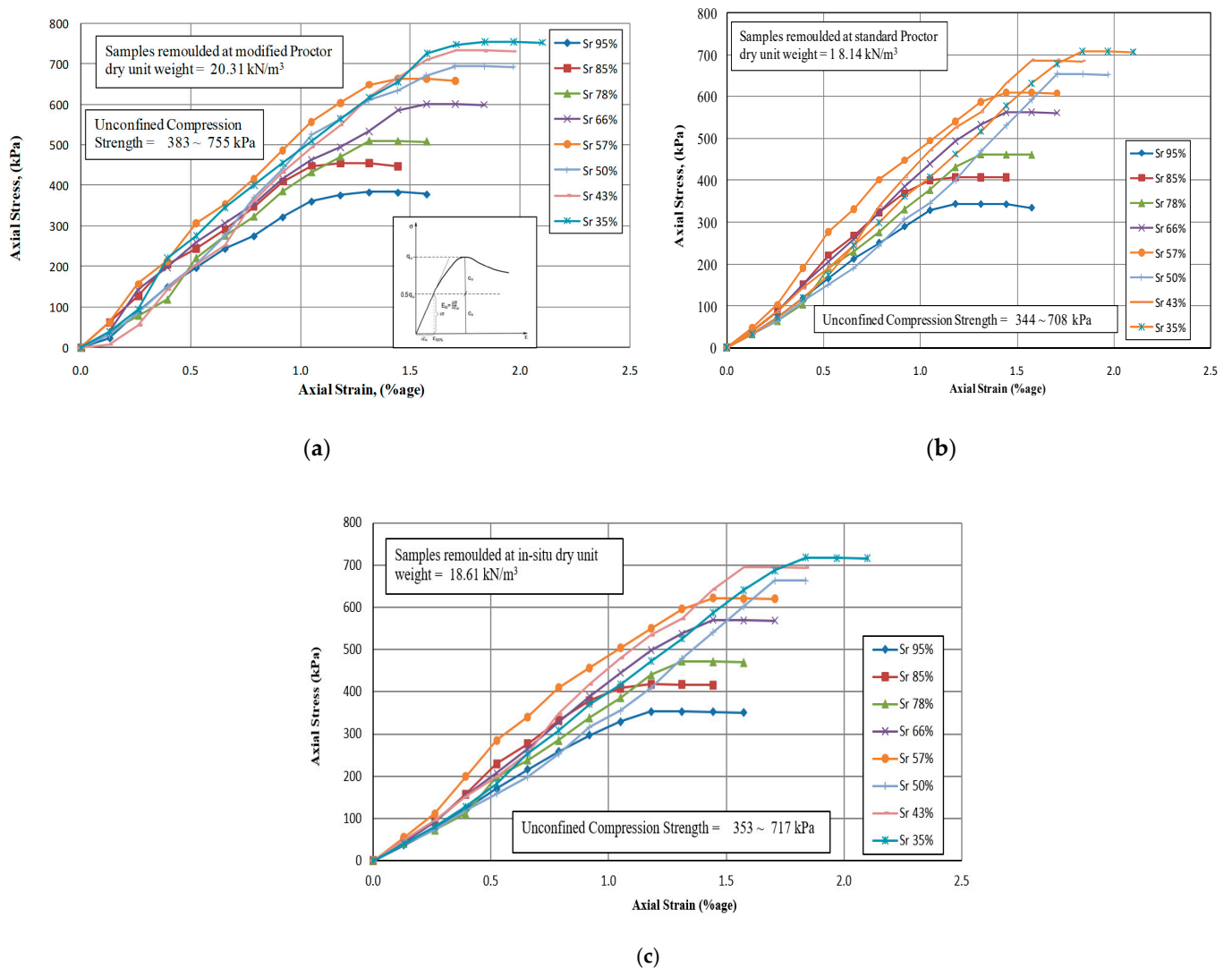


**Figure 7.** Stress versus axial strain of samples with varying degrees of saturation (35~95%) in an unconfined compression test remoulded at (a) Modified Proctor dry unit weight, (b) Standard Proctor dry unit weight, and (c) in-situ dry unit weight.

### 3.3. Jhika Gali Slope Stability Analysis

Slope stability analyses were performed by modeling the slope in GeoStudio software based on the determined shear strength parameters along the most likely failure plane. Figure 10 depicts a standard cross-section for landslide analysis.

Field observations and measurements, as well as information provided by the consultant National Engineering Services Pakistan (NESPAK, 2008), were used to predict the failure geometry [27]. Back analyses were used to determine the most likely surface that suited the observed physical restraints. The safety factor was computed for different values of dry unit weights, shear strength parameters, i.e., ( $c_u$  and  $\phi$ ) and saturations. The results of these analysis in Figure 11 shows that as the saturation increases, the factor of safety decreases dramatically and the slope becomes critical; furthermore, the factor of safety is reduced to below 1, somewhere between 85% to 95% degrees of saturation for various dry unit weights.

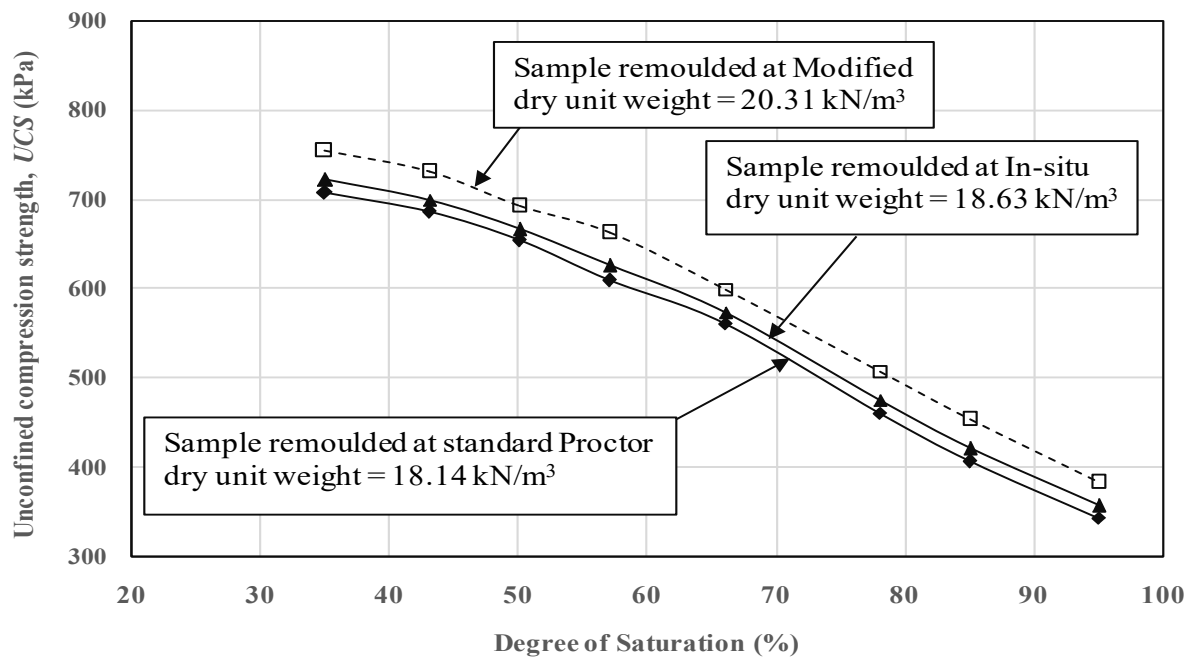


Figure 8. Degree of saturation vs. unconfined compression strength of samples remoulded to in-situ, standard and modified Proctor dry unit weights.

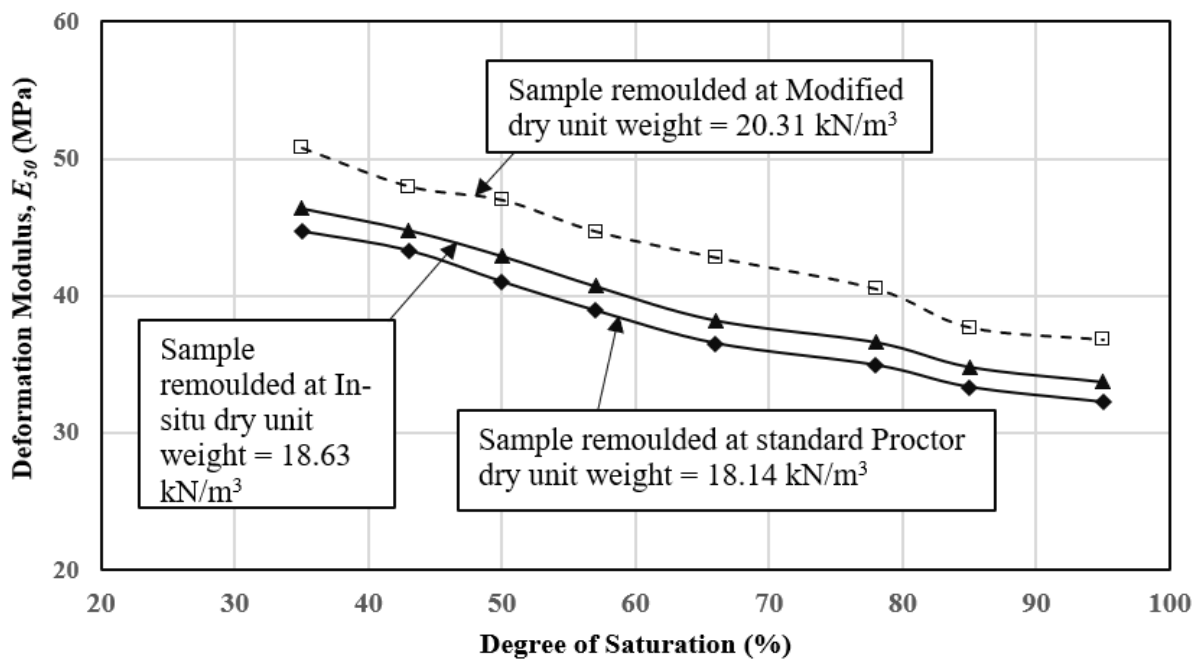


Figure 9. Degree of saturation versus deformation modulus of samples remoulded at in-situ, standard and modified Proctor dry unit weight.

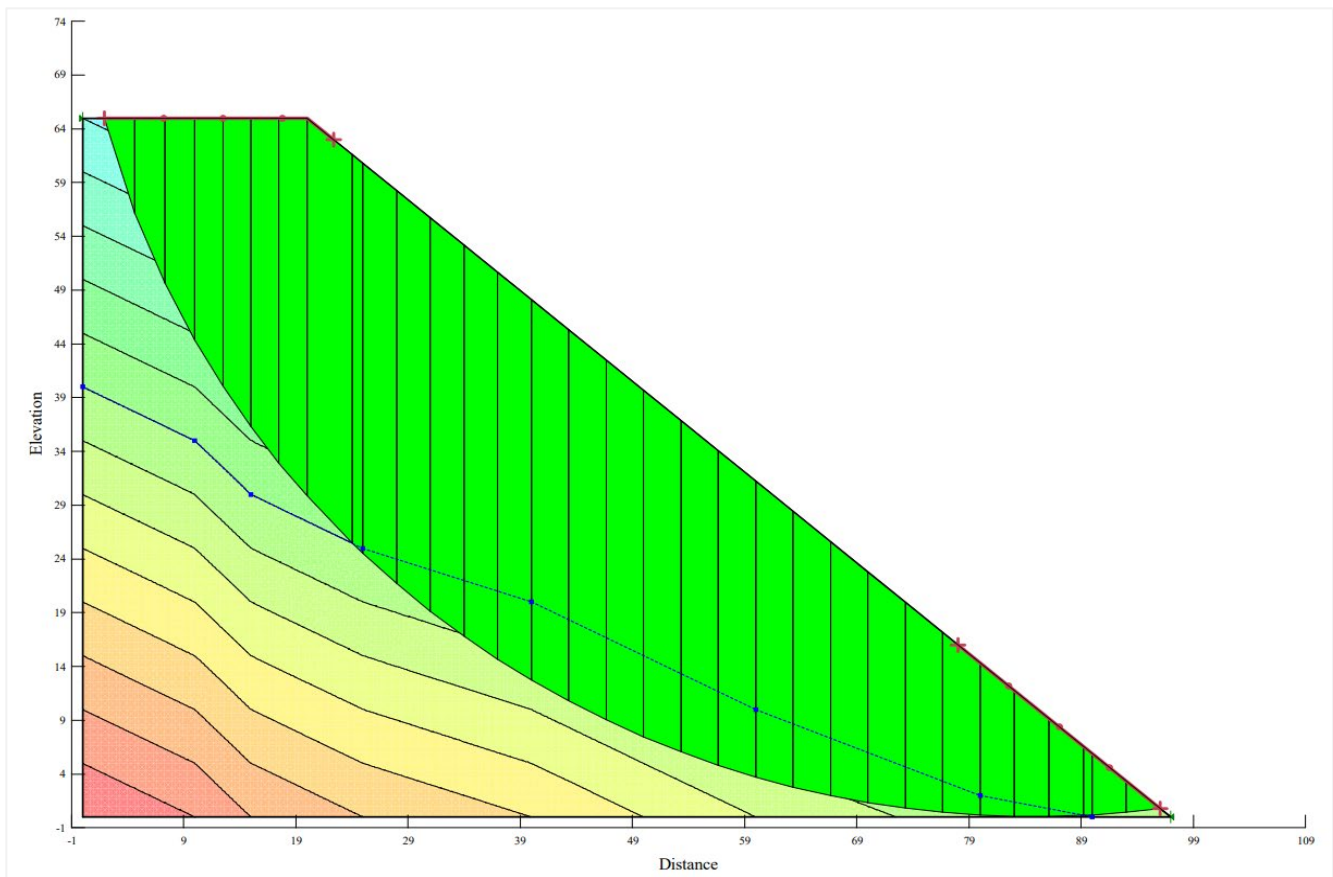


Figure 10. Jhika Gali slope modeled in GeoStudio for slope stability analysis for varying degrees of saturation.

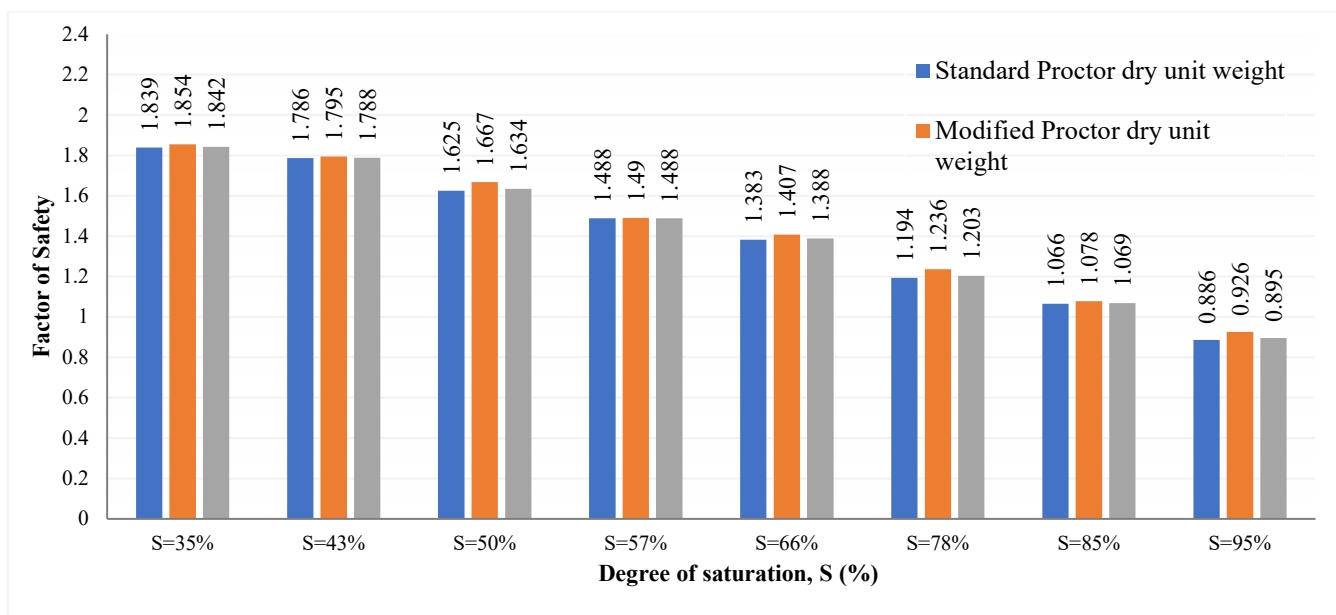


Figure 11. Factor of safety versus degree of saturation based on slope stability analysis.

#### Alteration in Slope Geometry for Stability

As the saturation increases above 85%, the factor of safety of the slope starts to reduce below one; at this stage the bulk unit weight of the material increases as compared to the

shear strength of the material and at 95% degree of saturation its value reaches 0.893, so this factor of safety indicates that the slope is in a critical condition and a landslide is most likely to occur. The factor of safety at this degree of saturation can be increased by altering the slope geometry in three different ways.

In the first case the height of the slope is reduced from 65 m to 55 m at an interval of 1 m and limit equilibrium analysis was performed on each reduction. After this alternation in slope geometry the critical factor of safety of slope at 95% degree of saturation increased from 0.893 to 1.042. Figure 12 shows the variation in the factor of safety with the reduction in the height of the slope.

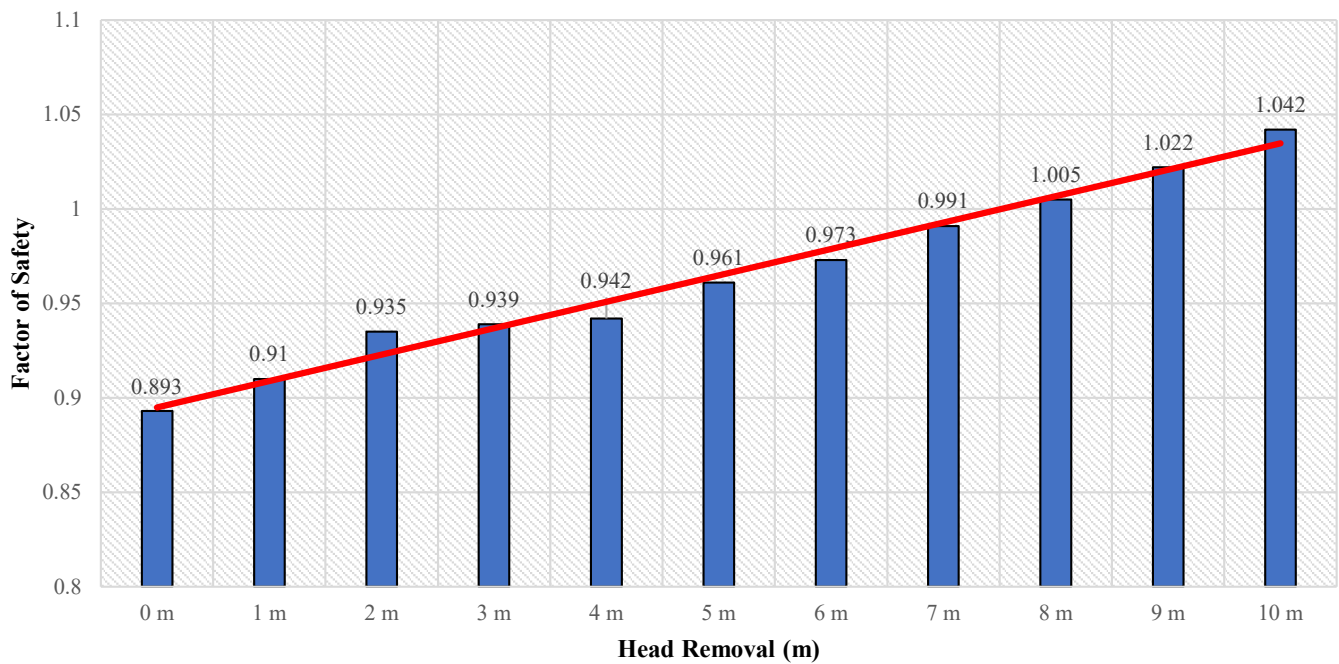


**Figure 12.** Effect of head removal on factor of safety of slope.

The slope geometry in the second case was changed by adding a counterweight at the toe from 1 m to 10 m in a limit equilibrium analysis. After this alternation the critical factor of safety of slope at 95% degree of saturation increased from 0.893 to 1.12. Figure 13 showed the increasing trend of the factor of safety with the increase in the counterweight. Slope alternation for the third case was done in the form of benching with varying slope angles from 50 degrees to 79 degrees; benching was done in one, two and three steps in a limit equilibrium analysis. Results showed that after this alternation in slope geometry the critical factor of safety of the slope at 95% degree of saturation increased from 1.017 to 1.307, 0.936 to 1.063 and 0.928 to 1.015 in one-step, two-step and three-step benching, respectively, and that now the slope is safe against sliding. Figure 14 showed the increasing trend of the factor of safety with the increase in the angle of benching and how one-step benching provides the highest factor of safety against sliding.

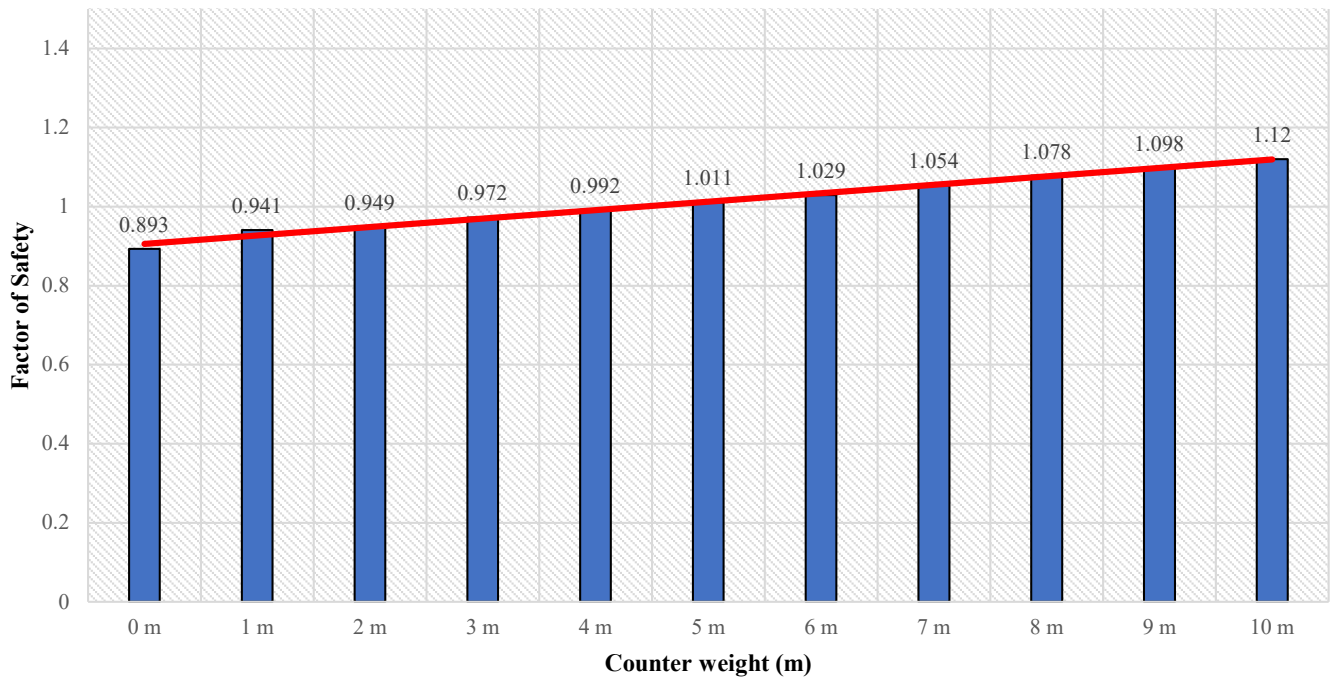


Figure 13. Effect of addition of counterweight at toe of slope on factor of safety of slope.

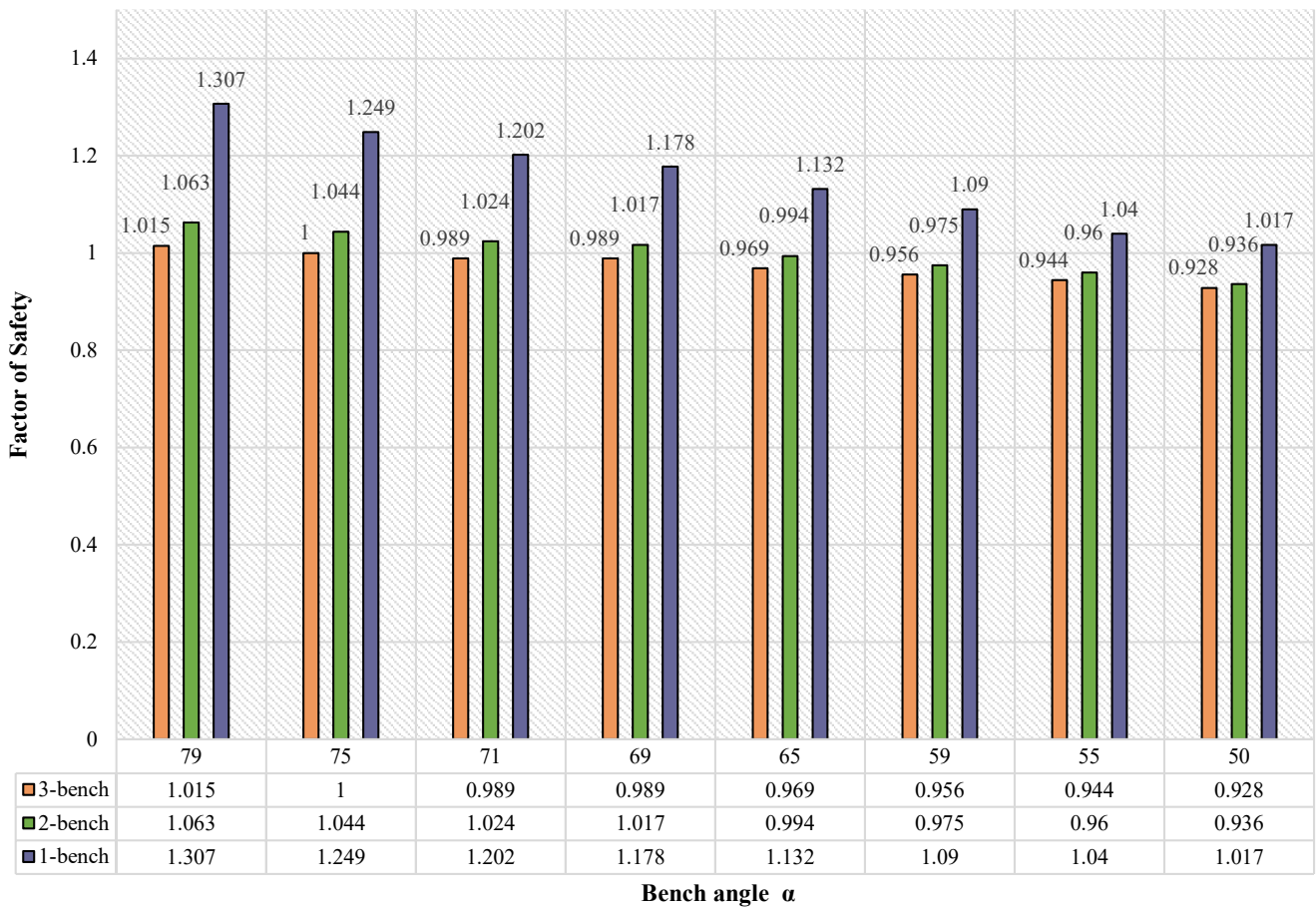


Figure 14. Effect of benching on factor of safety of slope.

#### 4. Conclusions

The main objective of this research was to look into the impact of saturation on the shear strength parameters of Jhika Gali and to assess the slope's stability. This investigation includes a detailed program of triaxial compression tests by changing the physical parameters of dry density and saturation. After this by using these parameters slope stability analysis was performed in GeoStudio for the determination of the factor of safety. In order to increase the factor of safety of the slope, alternation in the slope geometry was done. The following conclusion are summarized below.

- Based on the triaxial compression test results, it can be concluded that the undrained shear strength ( $c_u$ ) of the remolded samples at a particular degree of saturation increases by about 7~10% with the increase in dry unit weight. However, the cohesion decreases by about 51% as the degree of saturation increases from 35% to 95%. The friction angle ( $\phi$ ) improved approximately 6~11% with the increase in the dry unit weight at a specific degree of saturation, although the friction angle is reduced by about 41% as the degree of saturation is increased from 35% to 95%.
- According to a slope stability study conducted on GeoStudio, the landslides along the Jhika Gali road were caused by a reduction in the shear strength of the slide material due to a rise in saturation level. Consequently, with the increase in saturation levels the effective normal stress decreased along the slip surface. Stability analysis of the landslide shows that the factor of safety reduced from 1.854 to 0.886 as the saturation increased from 35% to 95%. When the saturation was about 85% to 95%, the slope was in the critical condition because of the low factor of safety.
- Landslide occurrence can be mitigated by flattening the slope geometry even when the degree of saturation is more than 85%. By reducing the height of the slope by about 10m the factor of safety is increased from 0.893 to 1.042. Similarly, by adding the counterweight at the toe of the slope by 10m the factor of safety increased from 0.893 to 1.12. In the last case by making the benches of the slope with angle variation the factor of safety increased from 0.893 to 1.307.
- The results of this study could be useful for a precise evaluation of possible landslides in other areas of Pakistan as well as in other parts of the world.

**Author Contributions:** Conceptualization, M.U.A. and H.M.; Data curation, M.U.A.; Formal analysis, M.U.A.; Funding acquisition, M.N.A., K.K. and M.I.F.; Investigation, M.U.A.; Methodology, M.U.A. and S.E.; Project administration, M.N.A. and M.U.A.; Resources, M.N.A. and K.K.; Software, M.U.A.; Supervision, M.N.A., H.M. and S.E.; Validation, H.M.; Visualization, H.M., S.E. and M.I.F.; Writing—original draft, M.U.A.; Writing—review & editing, H.M., S.E. and M.N.A. All authors have read and agreed to the published version of the manuscript.

**Funding:** This work was supported by the Deanship of Scientific Research, Vice Presidency for Graduate Studies and Scientific Research, King Faisal University, Saudi Arabia [Project No. GRANT1528]. The APC was also funded by "Project No. GRANT1528".

**Institutional Review Board Statement:** Not applicable.

**Informed Consent Statement:** Not applicable.

**Data Availability Statement:** The data used in this research have been properly cited and reported in the main text.

**Acknowledgments:** The authors acknowledge the Deanship of Scientific Research, Vice Presidency for Graduate Studies and Scientific Research, King Faisal University, Saudi Arabia (Project No. GRANT1528). The authors extend their appreciation for the financial support that made this study possible. This paper has also benefited from valuable comments and suggestions by anonymous reviewers, and our editor, whose efforts are gratefully acknowledged.

**Conflicts of Interest:** The authors declare no conflict of interest.

## References

1. Farooq, K.; Rogers, J.D.; Ahmed, M.F.J.E.S.R. Effect of Densification on the shear strength of landslide material: A Case Study from Salt Range, Pakistan. *Earth Sci. Res.* **2015**, *4*, 113. [[CrossRef](#)]
2. Mustafa, Z.U.; Ahmad, S.R.; Luqman, M.; Ahmad, U.; Khan, S.; Nawaz, M.; Javed, A. Investigating Factors of Slope Failure for Different Landsliding Sites in Murree Area, Using Geomatics Techniques. *J. Geosci. Environ. Prot.* **2015**, *3*, 39–45. [[CrossRef](#)]
3. Igwe, O.; Fukuoka, H. The effect of water saturation on the stability of problematic slopes at the Iva Valley area, Southeast Nigeria. *Arab. J. Geosci.* **2015**, *8*, 3223–3233. [[CrossRef](#)]
4. Salimi, S.; Yazdanjou, V.; Hamidi, A. Shape and Size Effects of Gravel Grains on the Shear Behavior of Sandy Soils. In *Landslides and Engineered Slopes. From the Past to the Future, Two Volumes+ CD-ROM*; CRC Press: Boca Raton, FL, USA, 2008; pp. 491–496.
5. Santoso, A.M.; Phoon, K.K.; Quek, S.T. Effects of soil spatial variability on rainfall-induced landslides. *Comput. Struct.* **2011**, *89*, 893–900. [[CrossRef](#)]
6. Kawamura, S.; Miura, S. Stability evaluation of slope with soft cliff. *Int. J. Geotech. Eng.* **2013**, *6*, 185–191. [[CrossRef](#)]
7. Khattab, S.A.; Al-Sulaifanie, B.J.; Alarna, A.M.M. Stability of unsaturated soil slopes subjected to external load and rainfall. *Int. J. Geotech. Eng.* **2018**, *15*, 633–641. [[CrossRef](#)]
8. Tsai, T.L.; Chen, H.F. Effects of the degree of saturation on shallow landslides triggered by rainfall. *Environ. Earth Sci.* **2010**, *59*, 1285–1295. [[CrossRef](#)]
9. Waseem, M.; Safdar, M.; ul Haq, T.; Shah, F.; Ahmad, W.; Ahmad, N.J.T.J. Slope Stability Analysis of the Qalandarabad Landslide. *Tech. J.* **2021**, *26*, 1–17.
10. Pasierb, B.; Grodecki, M.; Gwózdź, R. Geophysical and geotechnical approach to a landslide stability assessment. *Acta Geophys.* **2019**, *67*, 1823–1834. [[CrossRef](#)]
11. Yanrong, L. A review of shear and tensile strengths of the Malan Loess in China. *Eng. Geol.* **2018**, *236*, 4–10.
12. Xu, L.; Coop, M.R.; Zhang, M.; Wang, G. The mechanics of saturated silty loess and implications for landslides. *Eng. Geol.* **2018**, *236*, 29–42. [[CrossRef](#)]
13. Zhang, S.; Xu, Q.; Hu, Z.J.E.G. Effects of rainwater softening on red mudstone of deep-seated landslide. *Southwest China* **2016**, *204*, 1–13.
14. Ali, F.; Farooq, K.; Mujtaba, H.; Riaz, A.; Ulhaq, E. Influence of Saturation on Rainfall Generated Landslides in Shale along Murree-Kohala Road, Pakistan. *J. Geol. Soc. India* **2016**, *88*, 718–724. [[CrossRef](#)]
15. Ahmed, M.F.; Khan, M.S.; Raza, M.A.; Saqib, S.; Saadat, H. Slope failure analysis of Havelian landslide, Abbottabad Pakistan. *Pak. J. Sci.* **2016**, *68*, 462.
16. Ali, A.; Huang, J.; Lyamin, A.; Sloan, S.; Cassidy, M. Boundary effects of rainfall-induced landslides. *Comput. Geotech.* **2014**, *61*, 341–354. [[CrossRef](#)]
17. Li, W.C.; Lee, L.M.; Cai, H.; Li, H.J.; Dai, F.C.; Wang, M.L. Combined roles of saturated permeability and rainfall characteristics on the surficial failure of homogeneous soil slope. *Eng. Geol.* **2013**, *153*, 105–113. [[CrossRef](#)]
18. *ASTM D698-12(2021)*; Standard Test Methods for Laboratory Compaction Characteristics of Soil Using Standard Effort (12,400 ft-lbf/ft<sup>3</sup> (600 kN-m/m<sup>3</sup>)). ASTM International: West Conshohocken, PA, USA, 2021.
19. *ASTM D1557-12(2021)*; Standard Test Methods for Laboratory Compaction Characteristics of Soil Using Modified Effort (56,000 ft-lbf/ft<sup>3</sup> (2,700 kN-m/m<sup>3</sup>)). ASTM International: West Conshohocken, PA, USA, 2021.
20. *ASTM D2850-15*; Standard Test Method for Unconsolidated-Undrained Triaxial Compression Test on Cohesive Soils. ASTM International: West Conshohocken, PA, USA, 2016.
21. Morgenstern, N.U.; Price, V.E. The analysis of the stability of general slip surfaces. *Geotechnique* **1965**, *15*, 79–93. [[CrossRef](#)]
22. Farooq, K.; Orense, R.; Towhata, I. Deformation behavior of sandy soils during rainwater infiltration. *Soil Found.* **2004**, *44*, 15–30.
23. Farooq, K.; Orense, R.; Towhata, I. Response of unsaturated sandy soils under constant shear stress drained condition. *Soil Found.* **2004**, *44*, 1–13. [[CrossRef](#)]
24. Jonathan, W.; Rex, L.; Ning, L. Land sliding in partially saturated materials. *Hydrol. Land Surf. Stud.* **2009**, *36*, L02403. [[CrossRef](#)]
25. Kainthola, A.; Singh, P.K.; Singh, T.N. *Stability Investigation of Road Cut Slope in The Basaltic Rock Mass*; Geoscience Frontiers: Mahabaleshwar, India, 2014; pp. 1–9.
26. Kanwar, S.A. *Landslide Problems and Their Mitigation along Karakorum Highway*; Geological Survey of Pakistan Quetta: Quetta, Pakistan, 2006.
27. National Engineering Services (Pvt) Ltd. *Geotechnical Investigation Report for Construction of Car Parking Plaza at Jhika Gali, Murree*; NESPAK; National Engineering Services (Pvt) Ltd.: Lahore, Pakistan, 2008.